



# Experimental characterization of single droplets size and composition in liquid- liquid extraction systems with rainbow diffractometry

M. Ouattara, F. Lamadie, M. Sentis, F. Onofri

## ► To cite this version:

M. Ouattara, F. Lamadie, M. Sentis, F. Onofri. Experimental characterization of single droplets size and composition in liquid- liquid extraction systems with rainbow diffractometry. The International Symposia on Applications of Laser Techniques to Fluid Mechanics, Jul 2016, Lisbonne, Portugal. cea-02499788

**HAL Id: cea-02499788**

**<https://cea.hal.science/cea-02499788>**

Submitted on 5 Mar 2020

**HAL** is a multi-disciplinary open access archive for the deposit and dissemination of scientific research documents, whether they are published or not. The documents may come from teaching and research institutions in France or abroad, or from public or private research centers.

L'archive ouverte pluridisciplinaire **HAL**, est destinée au dépôt et à la diffusion de documents scientifiques de niveau recherche, publiés ou non, émanant des établissements d'enseignement et de recherche français ou étrangers, des laboratoires publics ou privés.

# Experimental characterization of single droplets size and composition in liquid-liquid extraction systems with rainbow diffractometry

M. Ouattara<sup>1,2</sup>, F. Lamadie<sup>1,\*</sup>, M. Sentis<sup>1</sup>, F.R.A. Onofri<sup>2,\*</sup>

1: CEA, DEN, DTEC, SGCS, F-30207 Bagnols-sur-Cèze, France

2: Aix-Marseille Université, CNRS, IUSTI, UMR 7343, 13453, Marseille, France

\* Correspondent authors: [fabrice.lamadie@cea.fr](mailto:fabrice.lamadie@cea.fr), [fabrice.onofri@univ-amu.fr](mailto:fabrice.onofri@univ-amu.fr)

**Keywords:** Liquid-liquid flows, Extraction, Droplets, Size, Composition, Rainbow scattering, Diffractometry

## ABSTRACT

This paper is focused on the analysis of the rainbow phenomenon produced by droplets with a low relative refractive index with the aim to characterize their size distribution and composition in liquid-liquid two-phase flows. The Lorenz-Mie theory, geometrical optics and physical approximations are used to bring insight on the specificities of the corresponding scattering patterns : near-forward location, reverse polarization and lower modulation compared to conventional rainbows. Material and methods to retrieve the parameters of the dispersed phase are reported when the rainbow diffractometry technique is operated as a single particle counting technique. Experimental results show that an accuracy better than 5% on the diameters and  $4 \cdot 10^{-1}$  on the refractive index (i.e. 0.8% in mass fraction of Marcol in hydrogenated tetrapropylene) can be achieved. These results open up perspectives for liquid-liquid extraction studies and more generally, mixing studies in two-phase flows.

---

## 1. Introduction

Liquid-liquid extraction, designed for selective separation of products in a mixture by solvent extraction, is a key process in chemical engineering. When applied in nuclear fuel reprocessing, two immiscible liquids are contacted: an aqueous phase and an organic phase. Only one phase, the continuous or the dispersed one, contains an extractant molecule capable of transferring the desired radioactive element from one phase to the other. After the transfer in a contactor such as a mixer-settler, an agitated or a pulsed column, both phases are separated by settling. To better understand the key factors and thus enhance the efficiency of the whole process, the experimental analysis of the kinetics of extraction and the interfacial area is a major issue, e.g. Lamadie *et al.* (2012). This requires in particular the determination of the size distribution and composition of the dispersed phase (i.e. in the present study, droplets with a low relative refractive index  $m \approx 1.06-1.23$ , the latter being used to infer the droplet composition).

For this purpose, in gas-flows and droplets with a large relative refractive index, the most promising elastic light scattering technique is certainly the rainbow or (global) rainbow

thermometry technique, e.g. Roth *et al.* (1990), van Beeck *et al.* (1999). However, surprisingly, this technique, that we prefer to call rainbow diffractometry (RD) for its obvious similarities with the forward diffractometry and critical diffractometry techniques (Onofri, 2012), has rarely been applied to the characterization of liquid-liquid systems, Lohner *et al.* (1999) and Vetrano *et al.* (2004). In the same way, the behavior of the rainbow phenomenon for droplets with a low relative index is not frequently discussed in the literature, e.g. Nussenzweig (1992).

From this assessment, this paper is focused on the analysis of the rainbow phenomenon produced by large droplets with a low relative refractive index with the aim to characterize liquid-liquid two-phase flows. It is structured as follows. After this introduction, section 2 briefly reviews the specificity of the rainbow pattern produced by droplets with a low relative refractive index. It shows that the Airy theory previously used to analyze liquid-liquid systems is not accurate enough for reliable measurements. Section 3 presents the material and methods, and more particularly the experimental setup, the calibration procedure of the RD system as well as the properties of the simulating fluids that are used for the liquid-liquid extraction process. Section 4 describes the rainbow signals post-processing, and the direct method developed for the retrieval of single-droplet parameters. Section 5 is an overall conclusion with perspectives.

## 2. Specificities of the rainbow scattering pattern of droplets with low relative refractive index

Following pure geometrical optics, the externally reflected rays ( $p=0$ ) and single internal reflected ( $p=2$ ) rays scattered at the rainbow angle  $\theta_r$  occurs for:

$$\begin{aligned}\theta_{p=0,r} &= 2\tau_{p=0,r} \\ \theta_{p=2,r} &= 4\tau'_{p=2,r} - 2\tau_{p=2,r}\end{aligned}\quad (1)$$

with  $\theta_{p=0,r} \equiv \theta_{p=2,r} \geq 0$ , where  $\tau_{2,r}$  and  $\tau'_{2,r}$  stand respectively for the complementary incident angle and the complementary refraction angle associated to the maximum deviation angle condition of rays  $p=2$ , with  $\tau_{2,r} = \sin^{-1}\left(\sqrt{(m^2 - 1)/3}\right)$  and  $\tau'_{2,r} = \cos^{-1}(\cos(\tau_{2,r})/m)$ , see van de Hulst (1957). Classically, in the latter equations, the relative refractive index  $m = m_2 / m_1$  is the ratio of the particle refractive index  $m_2$  in air, for the incident wavelength  $\lambda_0$ , and the corresponding refractive index  $m_1$  of the particle surrounding medium, see Fig. 1(a).

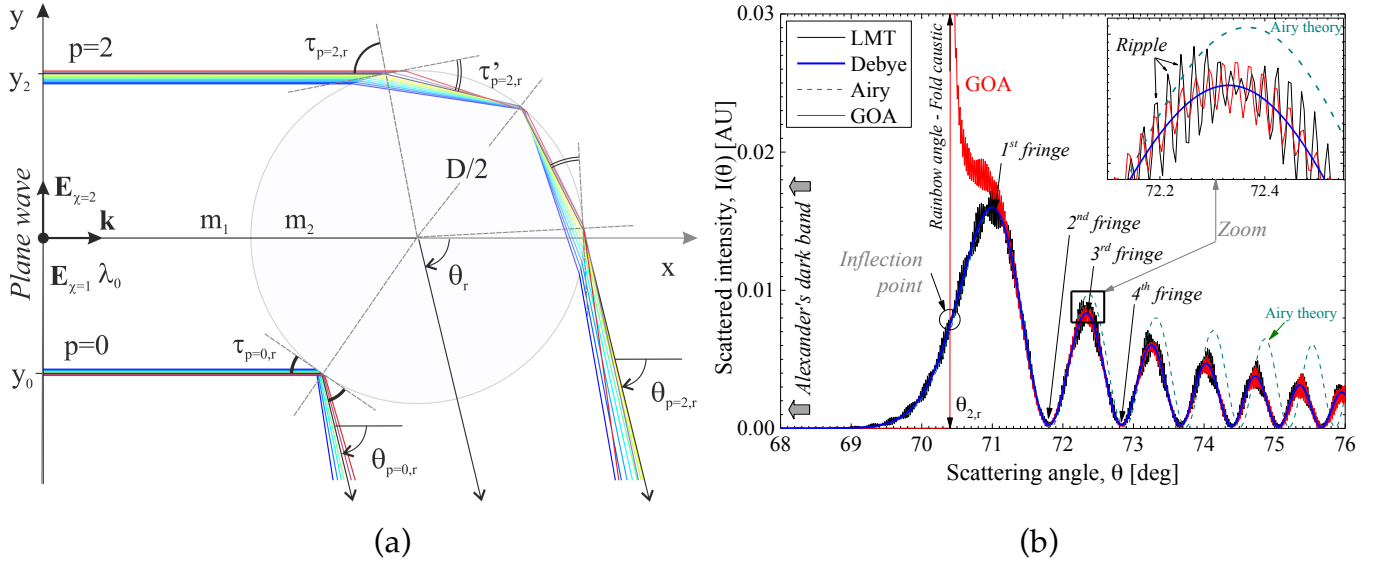


**Fig.1.** (a) Geometry and ray tracing calculations for the single internally refracted rays ( $p=2$ ) and externally reflected rays ( $p=0$ ) contributing the most to the first-rainbow pattern produced by a droplet with a low relative refractive index ( $m_2/m_1=1.06$ ); (b) comparison of the scattering diagram in the 1<sup>st</sup> rainbow angle region of a millimeter droplet with  $m=1.06$ , according to the Lorenz-Mie Theory (LMT, exact), the Debye theory (only partial waves  $p=2$ ) and Airy theory of the rainbow (i.e. physical optics approximation,  $p=2$  only), and an advanced Geometrical Optics Approximation (GOA) (rays  $p=0,1,\dots,8$ ). The zoomed view points out the ripple (high frequency) structures of the scattering pattern.

Using Eq. (1) we can readily show that for conventional rainbows, e.g. produced by liquid droplets in gas, the first rainbow is localized in the near-backward scattering domain ( $\theta_{2,r} \approx 137.8 - 157.2$  deg for  $m \approx 1.332 - 1.5$ ), whereas for common liquid-liquid systems ( $m \approx 1.06 - 1.23$ ), it is localized on the side-ways or in near-forward scattering regions ( $\theta_{2,r} \approx 57.3 - 93.5$  deg), see Fig. 1(b). In this angular region also takes place the Brewster angle  $\theta_{0,b}$  condition for the externally reflected rays and a parallel polarized incident beam (electrical field component  $\mathbf{E}_2$ , see Fig. 1(a)):

$$\theta_{0,b} = 2 \tan^{-1}(m^{-1}) \quad (2)$$

As illustrated on Fig. 2(a), for liquid-liquid systems, the two optical phenomena may coincide perfectly when  $\theta_{2,r} = \theta_{0,b}$ . Indeed, this condition occurs for a particular refractive index,  $m \approx 1.1005$  which can be estimated numerically by solving the former transcendental equation. This result is confirmed by Fig. 2(b) which presents the intensity of the partial waves  $p=2$  and  $p=0$  calculated with the Debye theory, for the parallel polarization and at the geometrical optics rainbow angle. To conclude on that point, contrary to droplets in gas-flows, the parallel polarization is the optimal one for low refractive index droplets. This polarization state of the

incident beam allows minimizing the relative contribution of the externally reflected rays to the rainbow signal, i.e. to minimize the amplitude of the ripple which contribution is often considered as disruptive, e.g. Saengkaew *et al.* (2010).

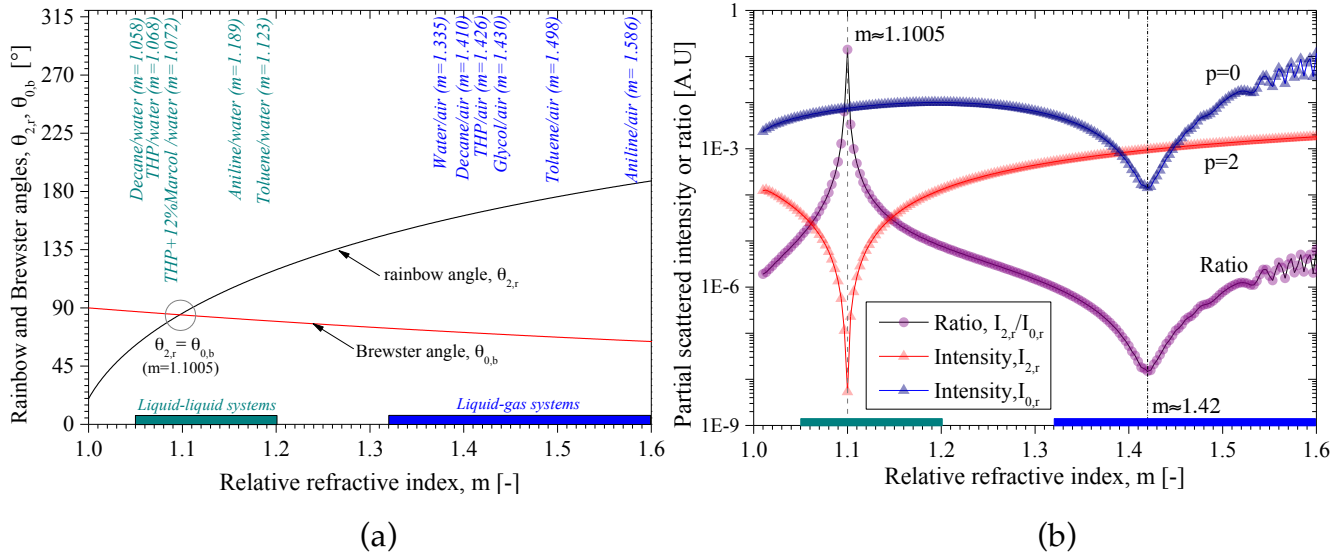


**Fig. 2** (a) Evolution of the geometrical optics positions of the rainbow and Brewster angles versus droplets relative refractive index. (b) Intensities and ratio of the partial waves  $p=2$  and  $p=0$  for the parallel polarization and at the geometrical optics rainbow angle (calculations performed with the Debye theory for droplets with diameter  $D=200\mu\text{m}$ ).

Going back to Fig. 1(b), it is also clear that the intensity decay and angular location of the supernumerary fringes ( $n \geq 2$ ) are poorly estimated by the Airy theory. This was confirmed by numerical calculations (not shown here) comparing the evolution of the angular position and intensity of the first supernumerary fringes for different droplet sizes. In fact, such a discrepancy, even for large droplets, is a third major difference with respect to droplets in gas-flows. Clearly, the predictions of the standard Airy theory are too rough (i.e. its angular range validity is limited) to be considered for the inversion of rainbow scattering patterns in liquid-liquid systems. In Fig. 1(b), excepted at the vicinity of the rainbow angle where takes place the caustic (Onofri *et al.*, 2015), the predictions of the GOA (Sentis *et al.*, 2016) appears to be in much better agreement with those of the Debye and LMT theories, for both the coarse and the ripple structures. One additional advantage of the GOA is that it can manage spheroidal droplets while being computationally efficient (Ren *et al.*, 2011). In any event, for convenience reasons, the LMT is used for all calculations presented in what follows and notably for the inversion procedure.

### 3. Experimental setup, fluids and calibration

The whole laboratory experiment is built around a column designed for liquid-liquid extraction studies, i.e. a rectangular tank equipped with four optical glass windows and filled with demineralized water, see Fig. 3. At the bottom of the tank, a needle produces a stream of single rising droplets (plus or less monodisperse) passing through the center of the probe volume, located 200 mm above the needle, i.e. along the z-axis (Lamadie *et al.*, 2012).

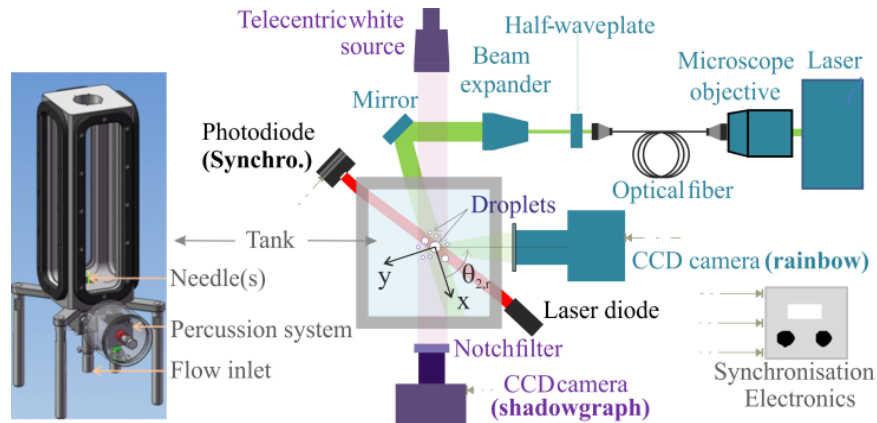


**Fig. 3** Schematic of the liquid-liquid extraction column and the optical setup (the optical measurements are performed 200mm above the needle).

The emission part of the RD-system is composed of a continuous high-power single-mode laser (doubled Nd:YAG 532nm, 5W) with a polarization maintaining beam delivery optics, a beam expander ( $\times 10$ ) and a half-wave plate. The beam expander allows to ensure that the beam waist is within the probe volume (defined as the crossing of all optical diagnostics field of views) as well as to enlarge the beam diameter up to  $2\omega_0 \approx 15\text{mm}$ . With a ratio of the beam diameter to maximum droplet size of  $2\omega_0/D_{\max} > 9$ , the latter condition allows minimizing Gaussian beam effects (as well as to characterize clouds of droplets, while these results are not reported in the present paper). The polarization optics is used to adjust the polarization (parallel) of the illumination beam. The detection of the RD-system is composed of a laser-line interference filter, a high-numerical aperture camera lens focused at infinite ( $f/d \# 1.4$ ), and a high resolution and high dynamic CCD camera (4MPix, 12 bits). A shadowgraph system is used for droplet size and shape comparison purpose. This system is composed of a white light source associated to a telecentric lens, a high magnification optics ( $\times 6.9\mu\text{m}/\text{pix}$ ) with a notch filter, a high resolution and high dynamic CCD camera (1.3MPix, 12 bits). Both systems are synchronized and triggered by a third optical system (basically a red laser diode and a photodiode) detecting all droplets passing within the optical probe volume which is common to both diagnostics, see Fig. 3.

**Table 1** Properties at 20°C and 1 atm. of the solutions used to generate droplets of various compositions.  
 \*when the surrounding fluid is composed of HPLC-grade water ( $m_1=1.3354$ ) -  $\lambda_0=532\text{nm}$ .

Properties	TPH (100%)	TPH (88%) + Marcol (12%)
Mass density [ $\text{kg.m}^{-3}$ ]	754.4	765.1
Dynamic viscosity [ $\text{Pa.s}$ ]	$1.10 \cdot 10^{-3}$	$1.94 \cdot 10^{-3}$
Surface tension [ $\text{N.m}^{-1}$ ]	0.04	0.04
Refractive index, $m_2$ [-]	1.4263	1.4315
Position of the 1 <sup>st</sup> rainbow*, $\theta$ , [deg]	70.7	73.2

For obvious reasons, activated fluids are not used in this preliminary study which goal is to investigate the potential of the RD for liquid-liquid extraction studies. Instead, various mixtures of Tetra-Propylene Hydrogenated (TPH) and Marcol are used as simulating fluids to produce the droplets. TPH is the diluent used with the solvent in the nuclear fuel recycling process, while Marcol is a saturated hydrocarbon liquid with a higher refractive index than TPH but with comparable viscosity and surface tension. In the same way, for the continuous phase, demineralized water (HPLC-grade) replaces the nitric aqueous solution used in the PUREX method. Nine solutions of TPH-Marcol mixtures were prepared to produce droplets with the aim to retrieve on-line their mixing fraction with the RD. Their mass fraction in Marcol is ranging from 0% to 12%, leading to absolute refractive indexes increasing from 1.4263 to 1.4315 (at 20°C) respectively. Some of their basic properties are summarized in Table 1. The refractive indexes of these solutions were carefully measured for a large range of temperatures (15-30°C) with an Abbe refractometer (resolution  $\pm 2 \cdot 10^{-4}$  at 532nm). For these conditions and the droplet sizes (600-1550 $\mu\text{m}$ ) considered here, the Eötvös and Reynolds numbers are in the range  $\#1.2 \cdot 10^{-1}$ - $2.6 \cdot 10^{-2}$  and  $\#6.4$ - $90.2$  ensuring a good sphericity of the droplets.

The angular calibration of the RD-system is obviously central to the method. As an order of magnitude, for a droplet with diameter  $D=1000\mu\text{m}$ , an error in the positioning of the detection system of 0.2deg would induce an error of  $\#5.7 \cdot 10^{-4}$  in the determination of its refractive index, i.e. an error of 1.3% on its volume fraction in Marcol. In order to minimize this error, the calibration of the RD-system is performed with a high resolution goniometer (embedding a

mirror submerged in the tank) and a careful auto-collimation procedure. For the experiments reported here, the pixel to angle calibration of this system is of  $6.10^{-3}$  deg/pix with a systematic error that is estimated to be lower than 0.05 deg (i.e. corresponding to a possible error of 0.3% in the fraction of Marcol over a maximum variation of 12%). Actually, the main source of uncertainty in this experiment lies in the control of the laboratory room temperature (and thus of both liquids). During an experiment, the variations of the latter were measured to be about  $\pm 0.5$ - $1^{\circ}\text{C}$  over 17 to  $23^{\circ}\text{C}$ . As the refractive index of the mixture varies almost linearly with the fraction of Marcol and the temperature, with respectively  $4.4 \cdot 10^{-4} / \%$  and  $4.6 \cdot 10^{-4} / ^{\circ}\text{C}$ , the variations of the laboratory room limit the expected resolution on the droplet composition to 0.5% in Marcol.

#### 4. Droplets parameters retrieval methods

The shadowgraph images are recorded using a short exposure time (less than  $80 \mu\text{s}$  considering that the velocity of droplets ranges from 3-7 cm/s) to minimize blurring effects. The shadowgraph images are characterized with a classical blob analysis followed by a linear interpolation scheme based on the point spread function of the high magnification optics.

The rainbow intensity profiles are obtained by averaging a 20 pixels central band height (i.e. off-axis angle range of  $\pm 0.15$ deg, see the embedded picture in Fig. 4(b)) from each image recorded by the corresponding CCD camera. This classical procedure allows to dump the contribution of the electronic white noise and thus to improve the SNR. For single droplets, in order to account for the CCD response (assumed to be linear) as well as to get a better graphical comparison with numerical calculations, the theoretical scattering diagrams are scaled to the experimental ones. The gain and offset are simply derived from the measurement of the intensity of the first and third supernumerary (bright) fringes. One further advantage of this scaling procedure, that was originally introduced to process critical-scattering patterns (Onofri *et al.*, 2009), is that it allows minimizing the effect of the variations of the rainbow signal intensity with the droplets trajectory within the probe volume. The droplets parameters (diameter and refractive index) are simply retrieved by comparing, in the least square sense, scaled experimental intensity profiles with theoretical intensity profiles calculated with the LMT (Onofri *et al.*, 2009). This procedure is illustrated in Fig. 4(a).



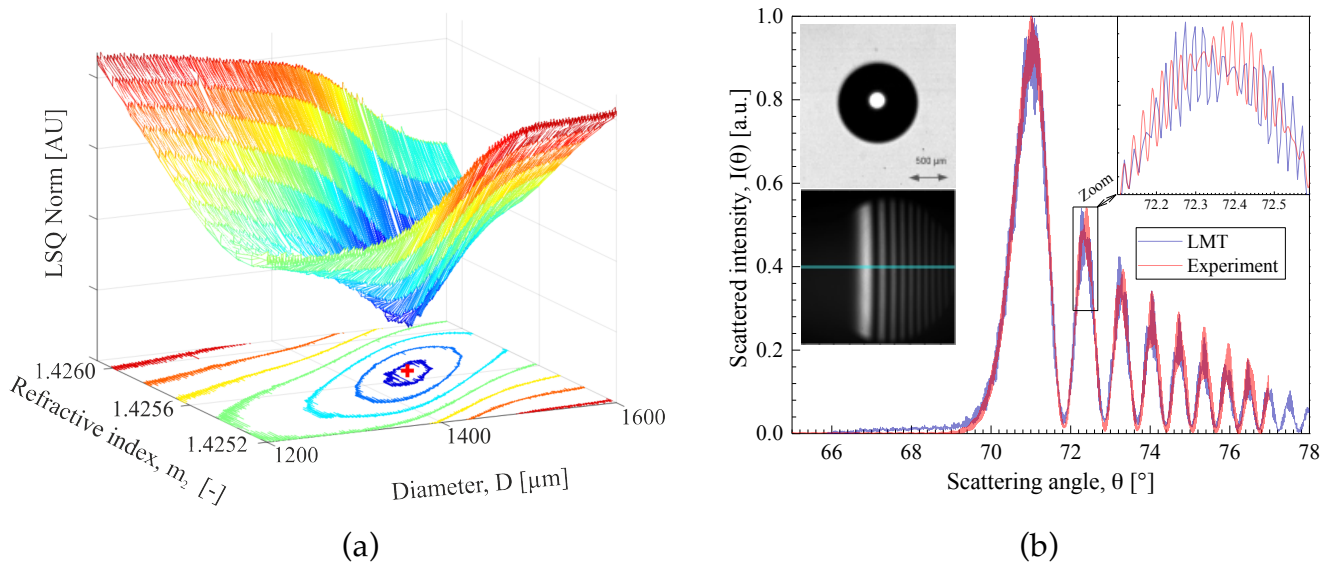
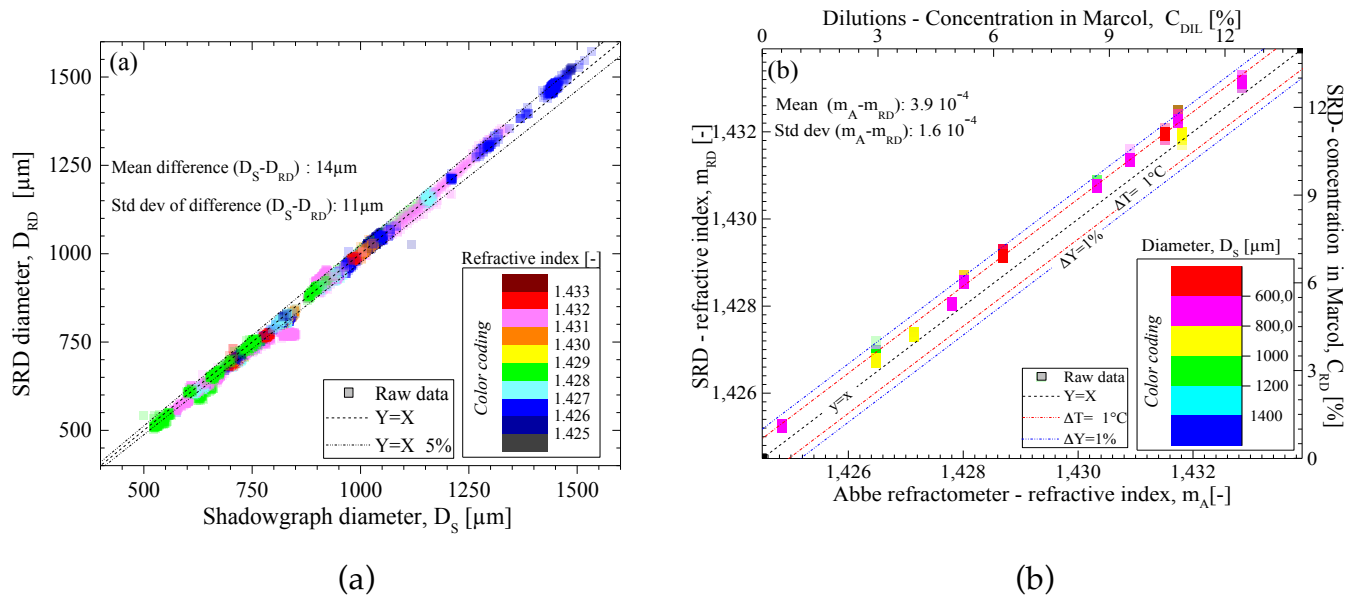


Fig. 4 (a) Typical evolution for the Euclidean norm ( $L^2$ ) of the least square difference between an experimental rainbow intensity profile and the profiles calculated with LMT for various sizes and refractive indexes. (b) Comparison of the experimental intensity profile and the reconstructed one (minimizing the norm of the least square difference). The corresponding shadowgraph image and rainbow scattering diagram are also shown.

## 5. Results and discussion

A typical shadowgraph image and the rainbow far field pattern of a free rising millimeter droplet containing 0% of Marcol are shown in Fig. 4(b), as well as the corresponding rainbow intensity profile and the reconstructed one. The two intensity profiles match pretty well. However, one can notice minor differences, like a small offset (more noticeable in the Alexander dark band) that is attributed to some residual background noise and a slight angular shift of the ripple. Three major reasons can easily explain this observation. Firstly, this shift could be attributed to small changes in the laboratory room temperature during the course of an experiment. Secondly, while the linearity and magnification of the shadowgraph system are quite limited, the aspect ratio of the largest droplets was estimated to be about 0.992 instead of 1 (spherical droplet model). It is known that even a small change in the droplets sphericity induces a shift of the ripple structure. Thirdly, any residual oscillations of the droplets cannot be rejected, even if such oscillations were not detected with the shadowgraph system. In any event, the droplet parameters retrieved,  $m_2 = 1.4253$  and  $D = 1015 \mu\text{m}$ , are in good agreement with the ones derived with the Abbe refractometer and the shadowgraph,  $m_2 = 1.4248$  and  $D = 995 \mu\text{m}$ . The values obtained with the RD are within the uncertainty of the values provided by the Abbe refractometer and the shadowgraph system.



**Fig. 5** (a) Comparison of the size of droplets with various compositions ( $m_2 = 1.4248 \sim 1.4317$ ) measured with the SRD and shadowgraph; (b) Comparison of the refractive index of droplets with various sizes ( $D = 600 \sim 1550 \mu\text{m}$ ) measured with the SRD and an Abbe refractometer (initial solutions). Both results correspond to 5700 analyzed droplets.

The results obtained for the nine solutions of TPH-Marcol mixtures are summarized in Fig. 5(a), which compares the droplet size measured with the shadowgraph and RD systems for various droplet compositions (color coding), while Fig. 5(b) compares the refractive index  $m_2$  measured by the Abbe refractometer and the RD system. Obviously, the RD provides simultaneously the size and refractive index of the droplets (5700 analyzed droplets). It is found that the global agreement on the droplet size is better than 5%, while the agreement on the refractive index is better than  $4 \cdot 10^{-4}$  (corresponding to an error on the estimation of the concentration in Marcoc of less than 0.8% or a change in the room temperature of less than  $1.1^\circ\text{C}$ ). The deviation in the slope of the linear regression is less than 1% in both cases with a correlation coefficient superior to 0.99.

## 6. Conclusion

The results presented in this paper clearly demonstrate the potential of the RD technique for the in-line analysis of the droplet size and composition in liquid-liquid systems. The LMT, geometrical optics and physical approximations are used to bring insight on the specificities of the corresponding scattering patterns: near-forward location, reverse polarization and lower modulation compared to conventional rainbows. Material and methods to retrieve the parameters of the disperse phase are reported when the rainbow diffractometry technique is operated as a single particle counting technique. Experimental results show that an accuracy

better than 5% on the diameters and  $4.10^{-4}$  on the refractive index (i.e. 0.8% in mass fraction of Marcol in TPH) can be achieved. These results open up perspectives for liquid–liquid extraction studies and more generally, mixing studies in two-phase flows. It will be shown in a forthcoming publication that the RD can also provide reliable statistics on liquid-liquid systems when it is operated as an ensemble averaging technique.

**Funding Information.** French National Research Agency (ANR) (ANR-13-BS09-0008-02, ANR-11-LABX-0092, ANR-11- IDEX-0001-0). This study is part of the “Nuclear Fuel Processing Program” of the French Alternative Energies and Atomic Energy Commission.

## References

- Lamadie F., Bruel L., Himbert M. (2012). Digital holographic measurement of liquid–liquid two-phase flows. *Optics and Lasers in Engineering* 50(12): 1716-1725.
- Lohner H., Lehmann P., Bauckhage K. (1999). Detection based on rainbow refractometry of droplet sphericity in liquid-liquid systems. *Appl. Opt.* 38(7): 1127-1132.
- Nussenzweig H.M. (1992). *Diffraction effects in semiclassical scattering*. Cambridge University Press, Cambridge.
- Onofri F., Barbosa S (2012), Chapter II: Optical particle characterization, in *Laser Metrology in Fluid Mechanics* (A. Boutier, ed.), Wiley-ISTE, London.
- Onofri, F. A., Krzysiek M., Mroczka J., Ren K.-F., Radev S., Bonnet J.-P. (2009). Optical characterization of bubbly flows with a near-critical-angle scattering technique. *Exp. in Fluids* 47(4-5): 721-732.
- Onofri F.R.A., Ren K. F., Sentis M., Gaubert Q., Pelce C. (2015). Experimental validation of the vectorial complex ray model on the inter-caustics scattering of oblate droplets. *Opt Express* 23(12): 15768-15773.
- Ren K. F., Onofri F., Rozé C. and Girasole T. (2011). Vectorial complex ray model and application to two-dimensional scattering of plane wave by a spheroidal particle. *Opt. Lett.* 36(3): 370-372.
- Roth N., Anders K., Frohn A. (1990). Simultaneous measurement of temperature and size of droplets in micrometer range. *J. of Laser. Appl.* 2(1 ): 37-42.
- Saengkaew S., Charinpanikul T., Laurent C., Biscos Y., Lavergne G., Gouesbet G., Gréhan G. (2010). Processing of individual rainbow signals. *Exp. Fluids* 48: 111-119.

- Sentis, M. P., Onofri F. R., Méès L., Radev S. (2016). Scattering of light by large bubbles: Coupling of geometrical and physical optics approximations. *J. Quant. Spectrosc. Radiat. Transfer* 170: 8-18.
- van Beeck J., Giannoulis D., Zimmer L., Riethmuller M. (1999). Global rainbow thermometry for droplet-temperature measurement. *Optics Letters* 24(23): 1696-1698.
- van de Hulst H.C. (1957). *Light scattering by small particles*, John Wiley & Sons.
- Vetrano M.R., van Beeck J.P.A.J., Riethmuller M.L. (2004). Global rainbow thermometry: improvements in the data inversion algorithm and validation technique in liquid–liquid suspension. *Appl. Opt.* 43(18): 3600-3607.